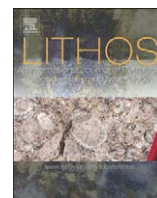




Contents lists available at ScienceDirect

Lithos

journal homepage: www.elsevier.com/locate/lithos

A major element, PGE and Re–Os isotope study of Middle Atlas (Morocco) peridotite xenoliths: Evidence for coupled introduction of metasomatic sulphides and clinopyroxene

Nadine Wittig^{a,*}, D. Graham Pearson^a, Joel A. Baker^b, Svend Duggen^{c,d}, Kaj Hoernle^c

^a Department of Earth Sciences, Durham University, South Road, Durham, DH1 3LE, UK

^b School of Geography, Environment and Earth Sciences, Victoria University of Wellington, P.O. Box 600, Wellington, New Zealand

^c Leibniz Institute of Marine Sciences, Kiel University, Wischhofstrasse, 1-3, 24148 Kiel, Germany

^d A.P. Møller Skolen—Upper Secondary School and Sixth Form College of the Danish National Minority in Germany, "Auf der Freiheit", 24837 Schleswig, Germany

ARTICLE INFO

Article history:

Received 9 March 2009

Accepted 2 November 2009

Available online xxx

Keywords:

Middle Atlas

Peridotite

Re–Os isotopes

Platinum-group elements

Mantle melting

Metasomatism

ABSTRACT

We present major element and PGE (platinum-group-element) abundances in addition to Re–Os isotope data for 11 spinel-facies whole rock peridotites from a single maar from the Middle Atlas Mountains, Morocco.

Major element systematics of these xenoliths are generally correlated with indices of depletion. FeO–MgO systematics appear to suggest spinel-facies melting in the range of 5 to 25%. However, Al₂O₃ abundances in these xenoliths appear elevated relative to primitive mantle (PRIMA). The Al₂O₃ abundances in conjunction with other major elements require distinct re-enrichment of the Middle Atlas continental mantle root due to melt/rock reaction and precipitation of amphibole and/or clinopyroxene from passing silicate melts akin to MORB or OIB that evolved in reverse direction along the melting curves in e.g. FeO–MgO space. Sc and V confirm the range of apparent depletion and also indicate that the currently preserved *f*O₂ in these peridotites is distinctly different from *f*O₂ conditions observed in subduction zones.

The majority of these xenoliths have low Os and Ir (I-PGEs) concentrations relative to PRIMA and modelled sulphide- and clinopyroxene-depleted residues of mantle melting under low *f*O₂, mid-ocean ridge-like conditions. Moreover, Pt and Pd (P-PGE) abundances are elevated when compared to their expected abundances after substantial melt extraction. Importantly, the systematically low Ir abundances in the majority of samples show well-correlated trends with Al₂O₃, MgO and Cu that are inconsistent with established melting trends. Os isotopes in the Middle Atlas xenoliths range from ¹⁸⁷Os/¹⁸⁸Os = 0.11604 to 0.12664 although most samples are close to chondritic. The Os isotope ratios are decoupled from ¹⁸⁷Re/¹⁸⁸Os but, together with Re abundances, also exhibit a good correlation with Al₂O₃, MgO and Cu.

The major element, I-PGE and Os isotope correlations suggest that the initial melt depletion led to the exhaustion of sulphide and clinopyroxene (20 to 30%) without significant stabilization of I-PGE-rich alloys. During later modal metasomatism of the refractory Middle Atlas continental mantle root with silicate melts akin to MORB or OIB the introduction of clinopyroxene/amphibole reduced the volume of the melt inducing sulphur saturation in these melts causing precipitation of secondary sulphides. This coupled crystallization of pyroxenes and sulphides (chalcopyrite) resulted in the two-component mixing systematics exhibited by I-PGEs, Os isotopes with major elements and Cu preserved in the Middle Atlas continental mantle root.

© 2009 Elsevier B.V. All rights reserved.

1. Introduction

Surprisingly little is known about the formation of the continental crust and its supporting mantle root in the Atlas region of North Africa (Fig. 1) although the lithospheric evolution is of considerable interest due to suspected petroleum deposits in the exposed marine

sediments. Geophysical examination associated with the exploration of these marine sediment deposits has revealed the Middle Atlas Mountain range as an inverted rift system (Beauchamp et al., 1996; Teixell et al., 2003; Ayarza et al., 2005). The neighboring Mediterranean has been studied more extensively and is known for its complex tectonic evolution in the Phanerozoic comprising Miocene subduction of the Alboran plate and the collision of Eurasia and Africa (e.g., Pearson et al., 1993; Duggen et al., 2003) while the West Africa Craton is situated further south and provides a tectonically stable platform. Consequently, knowledge of the age of the continental mantle root beneath the Middle Atlas region is highly desirable and may provide

* Corresponding author. GeoZentrum Nordbayern, Endogene Geodynamik, Schlossgarten 5, D-91054 Erlangen, Germany. Tel.: +49 9131 85 26 065; fax: +49 9131 85 295.

E-mail address: nadine.wittig@geol.uni-erlangen.de (N. Wittig).

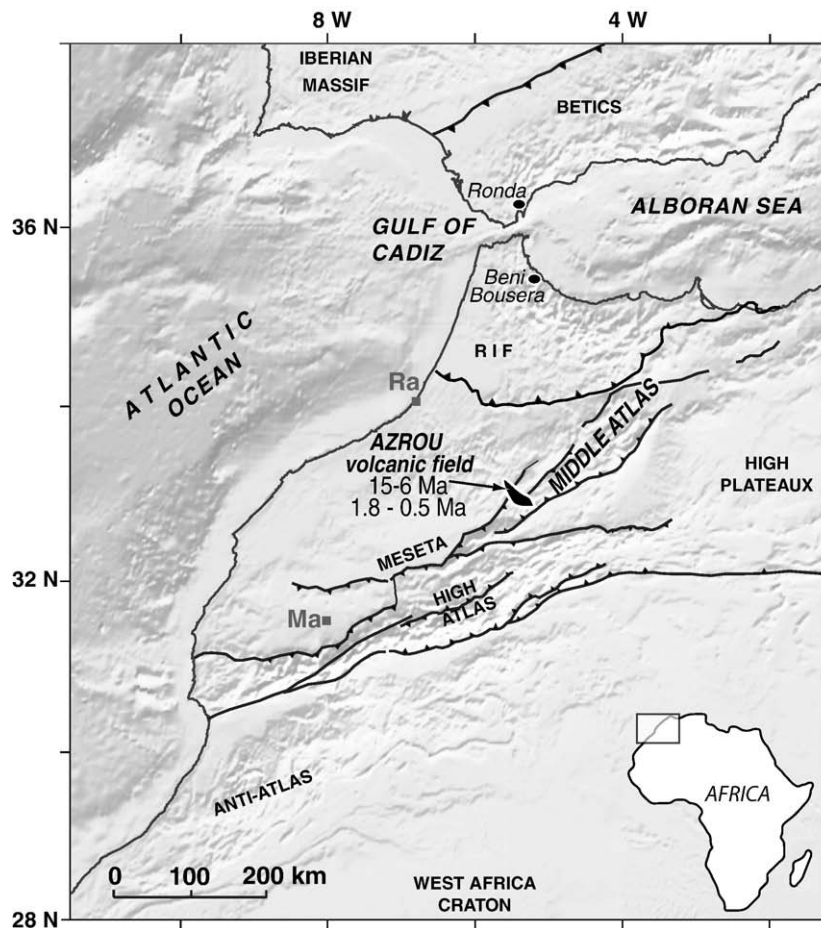


Fig. 1. Satellite image showing topographic features of northwest Africa. The samples investigated in this study were collected from the Azrou volcanic field in the Middle Atlas Morocco. Marrakech (Ma) and Rabat (Ra) are shown for orientation.

important information regarding the tectonic amalgamation of northwest Africa. Trace element and Sr–Nd–Hf–Pb isotope systematics of Middle Atlas clinopyroxenes from intraplate-basalt-borne peridotite xenoliths highlight the recent metasomatic history of this region, however, details of the initial depletion are not preserved in the lithophile trace element and isotope record (Wittig et al., 2008a, *in press*). Therefore, we endeavor to utilize concentrations of platinum-group elements (PGE) and Os isotope systematics of whole rock peridotites in order to, if possible, gain information of the timing of Middle Atlas SCLM (sub-continental lithospheric mantle) formation and the metasomatic evolution of this continental mantle root.

2. Geological setting and samples

The Atlas Mountain chain in Northwest Africa (Fig. 1) constitutes an approximately 2000 km long, ENE–WSW striking intra-continental orogenic belt ranging from Tunisia to Algeria (Saharan Atlas) to the continental margin of Morocco (High and Middle Atlas). The Middle Atlas branches off the High Atlas, trending over 250 km northeast toward the Mediterranean. The present-day Atlas Mountains comprise a number of failed rift basins associated with the Triassic–Jurassic opening of the central Atlantic and Neo-Tethys oceans. Convergence of Africa and Europe began in the Cretaceous and resulted in tectonic inversion of the Atlas rift, causing moderate crustal shortening of approximately 15 to 24% and exhumation of up to 4000 m (Gomez et al., 1998; Teixell et al., 2003; Ayarza et al., 2005; Zeyen et al., 2005). The continental crust in the Atlas rift is estimated to be less than 33 km thick and is marked by a comparatively shallow

MOHO with respect to the crustal shortening and high topography (Gomez et al., 1998; Teixell et al., 2003; Ayarza et al., 2005; Zeyen et al., 2005). Seismic studies have also revealed a relatively thin lithospheric mantle due to asthenospheric upwelling with the lithosphere–asthenosphere boundary being located at approximately 60–80 km depth (Teixell et al., 2003; Zeyen et al., 2005). The proposed lack of deeper lithospheric roots beneath the Atlas rifts coupled with high heat flow, a negative Bouguer anomaly, low seismic velocities in the SCLM, and intermediate depth earthquakes are thought to be suggestive of a recent SCLM delamination event (<20 Ma, Ramandi, 1998). These features of the inverted rifts in the Atlas region led Duggen et al. (2009) to propose sub-lithospheric channeling of the Canary plume toward the Middle Atlas region in order to explain the trace elemental and Sr–Nd–Pb characteristics of the volcanic rocks of this region. However, extremely deep, possibly cratonic SCLM (>200 km) has been recognized in the vicinity of the High Atlas and appears to extend further north toward the Middle Atlas region (Priestley and McKenzie, 2006). Consequently, SCLM delamination has to be a very localized phenomena, or is limited to the Rif region (Fig. 1). The contrasting information on the depth, age and nature of the Atlas lithosphere render the peridotite xenoliths from the Ibourhaltene maar particularly interesting in understanding the evolution of this portion of continental mantle root.

Approximately 100 intraplate volcanic vents are associated with the three dominant rift systems in Morocco (Fig. 1). Despite major interest in the Triassic–Jurassic formation of rift-associated supra-crustal rocks, the magmatic origin of the lithosphere is largely unconstrained. We are afforded a glimpse of the nature of the SCLM in this region by the presence of mantle xenoliths within the

Ibourhaltene volcanic event, located in the Azrou volcanic field (Duggen et al., 2009). The spinel-facies mantle xenoliths found here are coarse-grained, very fresh with no signs of serpentinization and generally exceed 15 cm in diameter. No garnet-bearing peridotites have been reported from the Middle Atlas thus far indicating a xenolith sampling depth of less than 80 km. The xenolith samples are generally lherzolitic with the exception of the highly refractory harzburgite Atl-3I, which contains ~90% olivine and only 2% clinopyroxene. On the other hand, the lherzolite Atl-3T contains ~23% clinopyroxene and comparatively little olivine (54%) rendering this xenolith the most fertile sample from the Middle Atlas studied here (Fig. 2). Sulphides are generally very rare (e.g. Atl-3F, Wittig et al., in press) or could not be detected during thin section examination. In thin section, the samples show no sign of strain or deformation except some kink-banding in olivine. The samples are generally granular and contain accessory amphibole inclusions in olivine and pyroxene. Orthopyroxene often hosts fluid and melt inclusions. Very rarely does amphibole occur in the form of porphyroblast relics (<1%, e.g., Atl-3F, Atl-3U, Atl-3L) that are associated with small pockets of in-situ melting. Clinopyroxenes from all Middle Atlas peridotites have enriched trace element systematics requiring the most recent enrichment to result from carbonatitic fluids. Sr–Nd–Hf–Pb isotopes are similar to present-day HIMU OIB although U/Pb and Th/Pb ratios are unusually high and indicate, in conjunction with Pb isotopes, very recent metasomatism (ca. 20 Ma, Wittig et al., 2008a, in press).

3. Analytical methods

Whole rock major and minor element analyses ($n=11$) were carried out at the X-ray fluorescence (XRF) spectrometer facility of the Grant Institute of Earth Science at the University of Edinburgh. The basaltic host rock was removed from the xenoliths using a Junior clipper saw at the Department of Earth Sciences at Durham University and approximately 300 g of peridotite was subsequently crushed in a fly press to obtain rock chips of <0.3 mm in diameter. Approximately 50 g of the well-mixed whole rock chips were then milled in an agate ball mill. The whole rock powder was then used for Os isotope and PGE determinations and an aliquot of ~10 g was sent to Edinburgh for analysis of major and trace elements (Table 1).

All PGE abundances were determined by isotope dilution techniques. Approximately 1 g of whole rock powder was combined with a

mixed PGE spike (^{190}Os , ^{191}Ir , ^{99}Ru , ^{194}Pt , ^{106}Pd and ^{185}Re) and attacked for ~12 h at 300 °C in an high pressure Asher (HPA-S, Anton Paar) utilizing ~2.5 mL 12 N HCl and ~5 mL 16 N HNO₃ (inverse Aqua Regia, iAR). Os was separated from other PGEs using carbon tetrachloride (CCl₄) and HBr. For further purification of Os a micro-distillation procedure was performed (Pearson and Woodland, 2000) and Os isotope ratios were measured using thermal ionisation mass spectrometry (TIMS) techniques in Durham. Details of the mass spectrometry procedures are given in Dale et al. (2008). The long-term Os isotope reproducibility (5 years) of the in-house Os isotope standard UMCP-3 is 4‰. A smaller number of the international Os isotope mass spectrometry standard DROsS (load size 0.1 ng, $n=7$) yields $^{187}\text{Os}/^{188}\text{Os} \sim 0.1608 \pm 5$, which is in excellent agreement with previously published data (Luguet et al., 2008). Replicate digestions of the in-house whole rock peridotite standard GP13 yields 1.7% reproducibility for Os isotopes and ~5% RSD for Os abundances ($n=10$, $^{187}\text{Os}/^{188}\text{Os} \sim 0.12605 \pm 19$, Os ~3.78 ppb), which is in excellent agreement with previously published data (Pearson et al., 2004). Total procedural Os blanks are <3 pg/g and insignificant considering the relatively high Os concentrations in these samples.

For determination of PGE abundances anion-exchange column procedures were performed (Pearson and Woodland, 2000). The samples were taken up in 10 mL of 0.5 N HCl and the sample matrix was eluted with 10 mL of 1 N HF/1 N HCl and 0.8 N HNO₃ before Ir, Ru, Pt and Re were collected in 10 mL of 13.5 N HNO₃. Pd was collected in 20 mL of 9 N HCl after a further 40 mL of 1 N HF/1 N HCl was administered. Both the Ir–Pt–Ru–Re and the Pd cuts were dried down, fluxed in 12 N HCl and taken up in 1 mL of 0.5 N HCl for mass spectrometry using the ThermoScientific Element2 ICP-MS in Durham. The reproducibility of Ir, Pt and Pd abundances in GP13 is ~10% RSD, whereas Re has an uncertainty of 3% RSD. Details of mass spectrometry procedures for Ir, Pt, Pd and Re are given in Dale et al. (2008), whereas Ru was run on a ThermoScientific Xseries2 ICP-MS. The alternative mass spectrometry routine for Ru utilizes second generation collision cell technology in order to eliminate Cr-based polyatomic interferences on ^{101}Ru , which may result in erroneously elevated Ru abundances if measurements are performed on the high resolution ThermoScientific Element2 ICP-MS (Meisel et al., 2008). A similar effect of high Cr abundances has previously been recognized during Rh ICP-MS concentration determinations (Krushevska et al., 2006). Ru abundances of GP13 derived from CCT-ICP-MS are in excellent agreement with previously determined data (Pearson et al., 2004) and yield a reproducibility of ~10% RSD.

4. Results

Major element and platinum-group element systematics and Re–Os isotope data for the Middle Atlas xenoliths are given in Table 1.

4.1. Major and minor element composition of Middle Atlas whole rock peridotites

The major element composition of the Middle Atlas peridotites ranges from more depleted to more enriched than primitive mantle (PRIMA, Walter, 2003). Generally, major element systematics are variable and well-correlated. For example, Al₂O₃ shows good correlations with TiO₂, Cr₂O₃, MgO, CaO and NiO (not shown). FeO is relatively constant and scatters around 8 wt.% whereas MgO varies from 38 to 47 wt.% (Fig. 3). Al₂O₃ and SiO₂ vary from 4.9 to 0.72 wt.% and 41.6 to 44.0 wt.%, respectively (Fig. 4). Ni abundances are typical for off-craton peridotites and correlate well with MgO and SiO₂ (Fig. 5). Similar relationships occur when Sc, V and Zn are plotted against MgO, FeO and SiO₂ (not shown). Sc and V abundances show a positive trend with each other (Fig. 6). Sample Atl-3T is generally different from the majority of peridotites in this study and resembles

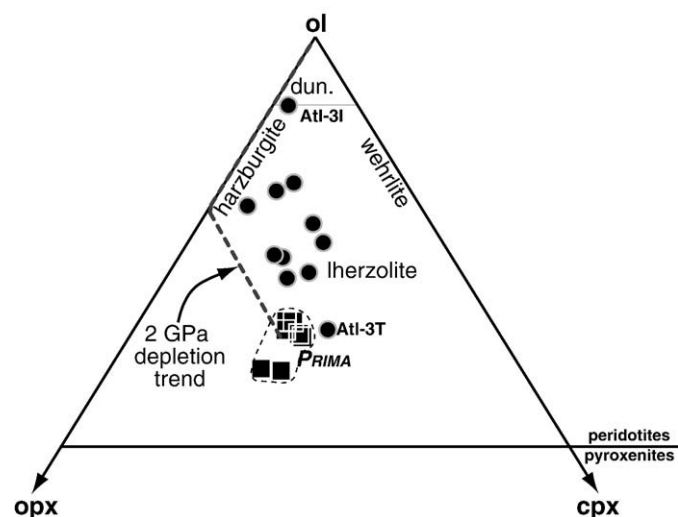


Fig. 2. Triangular plot of mineral modes from the Middle Atlas mantle xenoliths (black circles) after Streckeisen (1976). Also shown are different mode estimates of primitive mantle (PRIMA, black squares) after Walter (2003) and the mineralogical evolution of mantle residues after melting at 2 GPa (dashed grey line) evolving toward the dunite composition (dun.). Note the deviation of the Middle Atlas samples from the melting trend toward clinopyroxene. Samples Atl-3I and Atl-3T are highlighted.

Table 1
Mineral modes, major and minor element data, platinum-group element concentrations, Re–Os isotopes and T_{RD} model ages of Middle Atlas mantle whole rock xenoliths.

	Atl-3A	Atl-3B	Atl-3C	Atl-3E	Atl-3F	Atl-3I	Atl-3K	Atl-3L	Atl-3T	Atl-3U	Atl-3V
<i>Modal abundance (%)</i>											
ol	70	78	67	65	72	90	68	75	57	77	64
opx	14	13	20	18	14	7	21	20	20	16	21
cpx	16	8	12	16	13	3	11	4	23	7	14
spl	0.2	0.2	0.3	0.4	0.2	0.1	0.3	0.1	0.8	0.4	0.5
ol/opx	4.9	6.0	3.4	3.6	5.2	12.3	3.3	3.7	2.9	4.9	3.1
<i>Weight per cent</i>											
SiO ₂	43.97	42.74	43.87	43.92	43.99	41.56	43.91	43.57	43.68	43.40	43.69
TiO ₂	0.102	0.089	0.090	0.132	0.114	0.036	0.096	0.046	0.267	0.068	0.136
Al ₂ O ₃	2.18	1.98	2.69	2.92	1.99	0.723	2.36	1.44	4.88	1.87	3.11
Cr ₂ O ₃	0.301	0.378	0.350	0.351	0.306	0.252	0.295	0.249	0.667	0.283	0.381
FeO*	7.61	8.09	8.01	7.98	7.86	8.48	8.12	8.20	7.24	8.38	8.05
MnO	0.124	0.127	0.132	0.128	0.125	0.14	0.13	0.15	0.126	0.145	0.14
MgO	42.08	44.58	41.95	40.89	42.62	47.31	41.99	44.52	38.13	44.04	40.56
CaO	3.48	1.86	2.73	3.56	2.85	0.78	2.46	1.15	4.74	1.61	3.04
NiO	0.283	0.318	0.279	0.279	0.285	0.334	0.264	0.296	0.259	0.300	0.273
Na ₂ O	b.d.l	b.d.l	b.d.l	b.d.l	b.d.l	b.d.l	b.d.l	b.d.l	b.d.l	b.d.l	0.24
K ₂ O	0.011	0.014	0.051	b.d.l	0.003	b.d.l	0.032	0.008	0.191	0.047	0.116
P ₂ O ₅	0.008	0.001	b.d.l	b.d.l	0.002	0.016	0.006	b.d.l	0.051	0.005	0.020
SUM	99.57	99.48	99.53	99.53	99.56	99.47	99.76	100.68	99.30	99.57	99.79
LOI	−0.4	−0.2	−0.3	−0.3	−0.3	−0.9	−0.2	−0.3	1.8	−0.4	−0.3
Mg/Si	1.23	1.35	1.23	1.20	1.25	1.47	1.23	1.32	1.13	1.31	1.20
Al/Si	0.06	0.05	0.07	0.08	0.05	0.02	0.06	0.04	0.13	0.05	0.08
Ca/Al	2.15	1.27	1.37	1.65	1.94	1.46	1.41	1.08	1.31	1.16	1.32
Ca/Si	0.12	0.07	0.10	0.12	0.10	0.03	0.09	0.04	0.17	0.06	0.11
<i>Parts per million</i>											
Zn	46	59	53	52	49	64	53	56	53	60	61
Cu	9.6	38	19	16	7.0	2.4	10	4.1	11	3.6	19
Ni	2223	2498	2189	2195	2239	2622	2073	2323	2038	2357	2143
Cr	2062	2584	2397	2404	2095	1728	2019	1703	4568	1937	2604
V	63	49	58	73	54	20	55	34	111	42	71
Ba	5.5	39	5.3	2.9	3.2	2.9	62	18	148	13	37
Sc	15.2	11.1	12.9	15.6	12.0	3.3	11.8	6.4	19.3	9.5	13.4
<i>Parts per billion</i>											
Os	1.78	5.53	2.12	2.53	1.63	6.05	0.84	1.16	2.75	1.49	2.81
Ir	2.38	5.74	2.72	3.25	2.05	4.66	2.31	1.90	2.72	2.16	3.62
Ru	4.37	10.13	4.89	5.96	3.50	10.01	5.04	3.45	4.58	3.46	6.33
Pt	4.28	8.94	4.81	4.72	3.06	10.72	1.86	3.21	6.54	3.54	6.98
Pd	3.92	7.75	3.77	4.14	2.36	1.41	0.85	2.05	7.73	7.41	6.00
Re	0.044	0.271	0.091	0.084	0.013	0.004	0.058	0.014	0.328	0.025	0.110
Total PGE	17	38	18	21	13	33	11	12	24	18	26
Total I-PGE	9	21	10	12	7	21	8	7	10	7	13
Total P-PGE	8	17	9	9	5	12	3	5	14	11	13
[Re/Os] _N	0.41	0.80	0.70	0.55	0.13	0.01	1.12	0.19	1.94	0.28	0.64
[Ru/Ir] _N	1.18	1.13	1.15	1.18	1.09	1.38	1.40	1.16	1.08	1.03	1.12
[Pd/Ir] _N	1.36	1.12	1.15	1.05	0.95	0.25	0.31	0.89	2.35	2.83	1.37
[Os/Ir] _N	0.69	0.90	0.72	0.72	0.74	1.20	0.34	0.57	0.94	0.64	0.72
[Pt/Pd] _N	0.60	0.63	0.69	0.62	0.71	4.15	1.19	0.85	0.46	0.26	0.63
¹⁸⁷ Os/ ¹⁸⁸ Os	0.12232	0.12210	0.12492	0.12504	0.12244	0.11604	0.12280	0.12259	0.12463	0.12275	0.12664
1σ	0.00008	0.00005	0.00007	0.00006	0.00009	0.00005	0.00008	0.00007	0.00004	0.00007	0.00006
γOs	−1.7	−1.9	0.4	0.5	−1.6	−1.3	−1.5	0.2	−1.3	1.8	
¹⁸⁷ Re/ ¹⁸⁸ Os	0.119	0.236	0.208	0.161	0.128	0.004	0.157	0.023	0.192	0.068	0.562
T_{RD} (Ma)	901	938	541	523	884	1686	829	858	600	898	290

Notes: modal abundances of olivine (ol), orthopyroxene (opx), clinopyroxene (cpx) and spinel (spl) calculated after Kopylova and Russel (2000). FeO* is total Fe. LOI is loss on ignition. Below detection limit is b.d.l. The Os isotope deviation from the present-day ¹⁸⁷Os/¹⁸⁸Os of bulk earth is given in parts per cent as γOs (Meisel et al., 1996). PGEs were normalized to chondrite after McDonough and Sun (1995, Os = 490 ppb, Ir = 455 ppb, Ru = 710 ppb, Pt = 1010 ppb, Pd = 550 ppb and Re = 30 ppb).

or, is more fertile than, PRIMA (e.g., Al₂O₃, Figs. 3–6) whereas Atl-3I is consistently the most refractory peridotite.

4.2. Platinum-group element abundances and Re–Os isotope systematics in Middle Atlas whole rock peridotites

Platinum-group element (PGE) abundances in Middle Atlas whole rock peridotites are highly variable. I-PGE (Os, Ir, and Ru) are generally sub-PRIMA except for samples Atl-3I and Atl-3B, which yield total I-PGE abundances of >20 ppb (Fig. 7). The majority of samples have relatively high P-PGE abundances (Pt and Pd) that exceed those of I-PGEs and Re (Figs. 7 and 8).

Chondrite-normalized PGE patterns typically show increasing abundances from Os to Ru, lower Pt abundances and elevated Pd (Fig. 8). Fractionation of I-PGEs is substantial ([Os/Ir]_N = 0.34–0.94; chondrite is after McDonough and Sun, 1995). An exception is sample Atl-3I, which is marked by high Os abundances relative to Ir ([Os/Ir]_N > 1), low P-PGE and very low Re concentrations. Sample Atl-3K is also distinct from the majority of peridotites with markedly fractionated [Os/Ir]_N and low P-PGEs while Re, when normalized to chondrite, is higher than most PGEs. These two xenoliths and Atl-3B fall off the otherwise tight correlations formed by I-PGEs, particularly Ir, with MgO, Al₂O₃ and also Cu (Fig. 9). The Middle Atlas xenoliths have PGE patterns similar to those of Vitim xenoliths (Pearson et al., 2004), although the

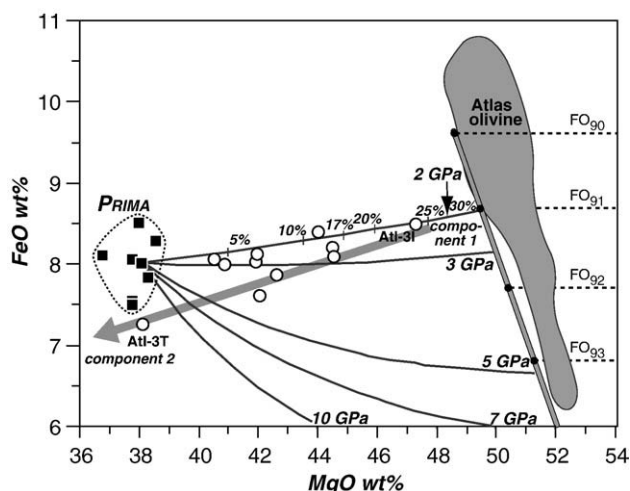


Fig. 3. FeO versus MgO (wt.%) of whole rock peridotites of Middle Atlas peridotite xenoliths. Residue evolution for melting beginning at 2, 3, 5, 7 and 10 GPa, and olivine composition with respect to Mg# (open circle, grey band) is taken from Herzberg (2004). PRIMA compositions (black squares) are taken from Walter (2003). Middle Atlas olivine compositions are taken from Wittig (2006). Also shown is a vector trending from the most depleted sample Atl-3I to the composition of clinopyroxene and amphibole.

Middle Atlas samples have less fractionated $[Os/Ir]_N$ and show stronger Pd enrichment.

Os isotope compositions range from $^{187}Os/^{188}Os$ 0.11604 to 0.12664 and do not correlate with $^{187}Re/^{188}Os$ (0.0035 to 0.568, Fig. 10). Notably, half of the samples studied have $^{187}Os/^{188}Os$ of ~ 0.122 that yield T_{RD} model ages (Walker et al., 1989) of ~ 1000 Myr, whereas the remaining samples have more radiogenic, but variable Os isotopes. Only sample Atl-3I exhibits relatively unradiogenic Re–Os isotope systematics ($^{187}Os/^{188}Os \sim 0.116$, Fig. 10). The Re abundances and Os isotope ratios of these xenoliths correlate very well with Al_2O_3 (Fig. 10).

5. Discussion

5.1. Major element correlations: evidence for initial melt extraction or secondary modal metasomatism in Middle Atlas mantle xenoliths?

When considering the variation of major elements in relation to the initial melting depths, combined FeO–MgO systematics provide

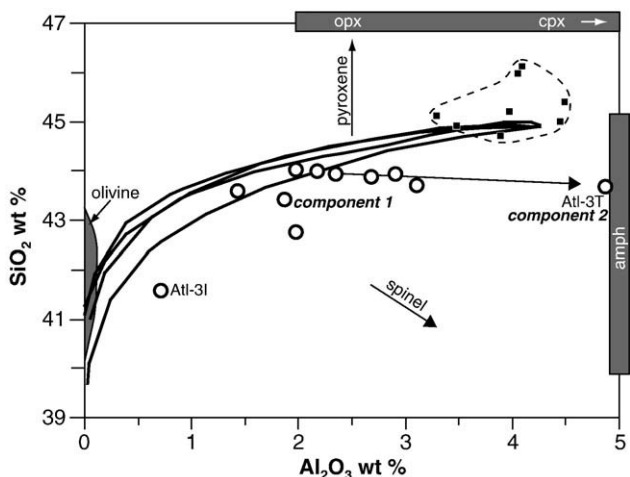


Fig. 4. SiO_2 versus Al_2O_3 (wt.%) of whole rock peridotites from Middle Atlas mantle xenoliths. Residue evolution for melting beginning at 2, 3, 5, 7 and 10 GPa is taken from Herzberg (2004). Also shown is the composition of constituent olivine and the range of pyroxene, spinel and amphibole is indicated (Wittig, 2006). Note the relatively constant SiO_2 and variable Al_2O_3 , which may suggest precipitation of amphibole and/or spinel-clinopyroxene at the expense of olivine. PRIMA compositions (black squares) are taken from Walter (2003).

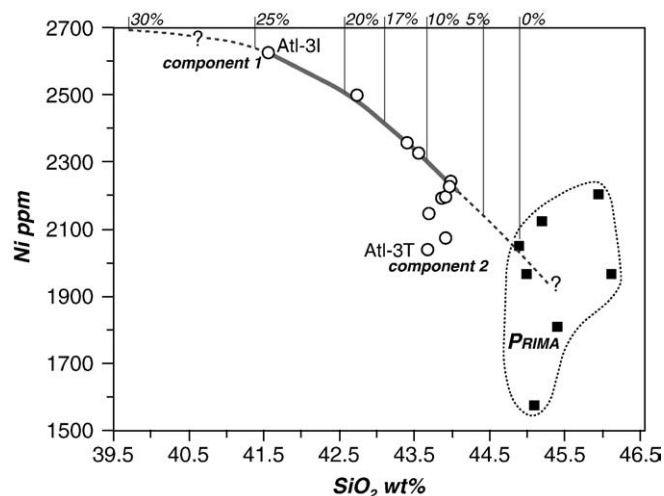


Fig. 5. Ni (ppm) versus SiO_2 (wt.%) of whole rock peridotites from Middle Atlas mantle xenoliths. Also shown is a mixing line from PRIMA compositions (black squares, Walter, 2003) to the most depleted sample Atl-3I. Degree of depletion derived from SiO_2 is projected onto the PRIMA–Atl-3I correlation by using the polybaric residue evolution at initial melting pressure of 2 GPa (Herzberg, 2004). Note the large uncertainty of Ni concentrations in PRIMA.

the best distinction between residues resulting from shallow initial melting depths (i.e. 2 to 3 GPa, Walter, 1999; Herzberg, 2004; Ionov and Hofmann, 2007) and those with deeper origin of melting (e.g. 7 GPa). For example, Middle Atlas xenoliths have FeO and MgO relationships that plot along a ~ 2 GPa melt residue trend indicating 5 to 25% melt extraction, although some scatter is evident (Fig. 3). Considering such a spinel-facies melting scenario, Sc and V abundances confirm the range of apparent melt extraction and indicate fO_2 conditions ($\sim NNO - 1$ to -2 , Fig. 6) similar to those anticipated for abyssal peridotites (Canil, 2002, 2004). This suggests that if melt extraction caused the correlation of Sc and V, this depletion occurred in an environment characterized by fO_2 conditions akin to present-day mid-ocean ridges.

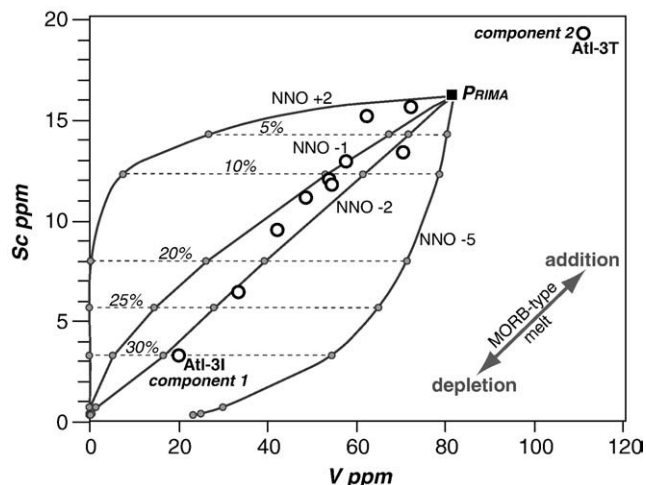


Fig. 6. Sc versus V in parts per million of whole rock peridotites from Middle Atlas mantle xenoliths. Also shown are residue evolution lines for 1.5 GPa isobaric melting using different fO_2 (Canil, 2002) ranging from NNO+2 to NNO-5 beginning at PRIMA (McDonough and Sun, 1995). Stippled lines indicate 5, 10, 20, 25 and 30% melt extraction. Note that this isobaric model may overestimate the degree of depletion, which may result from a) over-estimation of phase stability during mantle melting, or b) the robustness of Sc and V against ubiquitous metasomatic enrichment. The Middle Atlas xenoliths suggest depletion under fO_2 conditions (NNO-2) similar to those estimated for mid-ocean ridges. Mantle minerals precipitated from MORB- or possibly OIB-type melts may result in addition of Sc and V along the same trajectory in reverse direction.

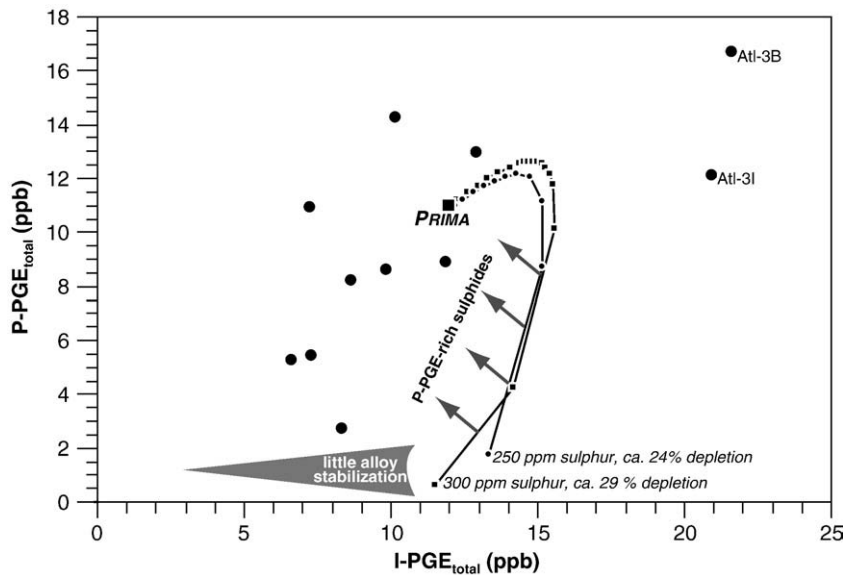


Fig. 7. P-PGE versus I-PGE in parts per billion of Middle Atlas whole rock peridotites (closed circle). The residue evolution of PRIMA is shown in 1% increments (after Pearson et al., 2004) for PRIMA sulphur contents of 250 and 300 ppm. Also shown is the anticipated effect of introduction of interstitial metasomatic P-PGE-rich sulphides. Middle Atlas peridotites are marked by elevated P-PGE abundances that are distinct from the depletion trend. Exceptions are Atl-3B and Atl-3I, which are enriched in P- and I-PGEs.

However, a mildly incompatible major element oxide such as Al_2O_3 , in combination with SiO_2 , which is most sensitive to the metasomatic consumption of olivine and the subsequent precipitation of pyroxene (Kelemen et al., 1998) and/or amphibole, reveal significant scatter when plotted together with residue curves of polybaric melting. Wittig et al. (2008b) have shown that such elemental systematics in peridotites that have been modally metasomatised cannot be used to estimate the depth of melting. In fact, in Al_2O_3 – SiO_2 space the residue curves for different initial melting pressures plot close together and are insensitive to determining initial melting depths. In the case of the Middle Atlas xenoliths it is clear that Al_2O_3 is elevated at a given SiO_2 (Fig. 4). This Al_2O_3 – SiO_2 range may be best explained by the precipitation of minor amounts of amphibole (~15 wt.% Al_2O_3 , 40 to 45 wt.% SiO_2). Alternatively, introduction of very Al-rich, but modally insignificant clinopyroxene (Wittig, 2006, up to 16 wt.% Al_2O_3 , ~50 wt.% SiO_2) that is distinct from primary chrome-diopside (<<6 wt.% Al_2O_3 , ~51 wt.% SiO_2) could account for the enhanced Al_2O_3 observed in these peridotites. Currently the Middle Atlas xenoliths contain only minor amounts of amphibole and the samples displaying the greatest enrichment in Al_2O_3 contain the least amount of amphibole. In these samples amphibole occurs as rare inclusions in olivine and pyroxenes (e.g., Atl-3T and Atl-3V, Wittig, 2006) suggesting that the amphibole was formed and later partially reacted to form spinel and clinopyroxene prior to sampling by the host volcanic rocks and eruption. A similar reaction has been reported from Eifel peridotite xenoliths (Ban et al., 2005) in conjunction with small degree melting. The previous existence of higher modal amounts of amphibole or Al-rich clinopyroxene can also be reconciled with the whole rock FeO–MgO systematics, because the same samples that exhibit the highest abundances of “amphibole-component” also form a trend towards the FeO–MgO composition of the pyroxenes and amphibole (Fig. 3). We take the elevated whole rock Al_2O_3 contents and other aspects of the major element systematics to mean that these peridotites probably experienced some form of modal enrichment after the initial depletion. As such, the estimated 5 to 25% melt extracted should be considered minimum values when constraining the initial degree of melt depletion. Moreover, silicate minerals such as clinopyroxene and amphibole that precipitate from passing basaltic melts are significant sinks for transition metals such as Sc and V (Canil, 2002, 2004). Consequently, the robustness of Sc and V (Canil, 2002, 2004) as an indicator of $f\text{O}_2$ of a respective depletion setting has to be

questioned in samples that may have experienced modal metasomatism due to this type of enrichment. Furthermore, we have to recognize that the introduction of Al_2O_3 -bearing phases such as clinopyroxene and amphibole into the peridotite matrix due to silicate melt metasomatism may be associated with the introduction of sulphides (Lorand et al., 2003). Such a metasomatic scenario also has implications for the meaning of Al–Os isotope correlations, i.e. aluminachron, that are often observed in off-cratonic continental mantle roots. These Os–Al correlations are frequently used to estimate SCLM formation ages (Reisberg and Lorand, 1995; Rudnick and Walker, 2009). Hence, this contribution will focus on the relationship of major elements with PGEs and Os isotopes of modally metasomatised SCLM such as the Middle Atlas continental mantle root.

5.2. A PGE approach to mantle melting under low $f\text{O}_2$ conditions

As outlined earlier, the initially depleted Middle Atlas xenoliths most likely experienced modal enrichment resulting in clinopyroxene-spinel and/or amphibole precipitation (subsequently recrystallizing to clinopyroxene-spinel). This means that, as in cratonic peridotites (Simon et al., 2003), at least a portion of the clinopyroxenes in these xenoliths may be of secondary origin and, clearly, analysing these clinopyroxenes for their lithophile element and isotope composition will not reveal details of mantle melting processes. For example, in these clinopyroxenes neither the most robust lithophile trace elements abundances of Lu and Hf, nor their isotope ratios are indicative of mantle melting (Wittig et al., 2008a). Different geochemical proxies must be utilized to investigate the depletion mechanisms that effected this continental mantle root.

Re–Os isotopes have been shown to preserve information regarding the timing of initial depletion and stabilization of cratonic lithospheric mantle (e.g. Kaapvaal, Slave and North Atlantic Craton, Pearson and Wittig, 2008 and references therein). The PGE systematics in these Archean SCLM roots are marked by extreme P-PGE depletion that is taken as evidence of mantle melting (Pearson et al., 1995; Irvine et al., 2001, 2003; Pearson et al., 2004). Clearly, examining PGE systematics in conjunction with Os isotopes in off-cratonic SCLM such as the Middle Atlas xenoliths may hold the potential to characterize mantle melting events (Handler and Bennett, 1999; Rudnick and Walker, 2009).

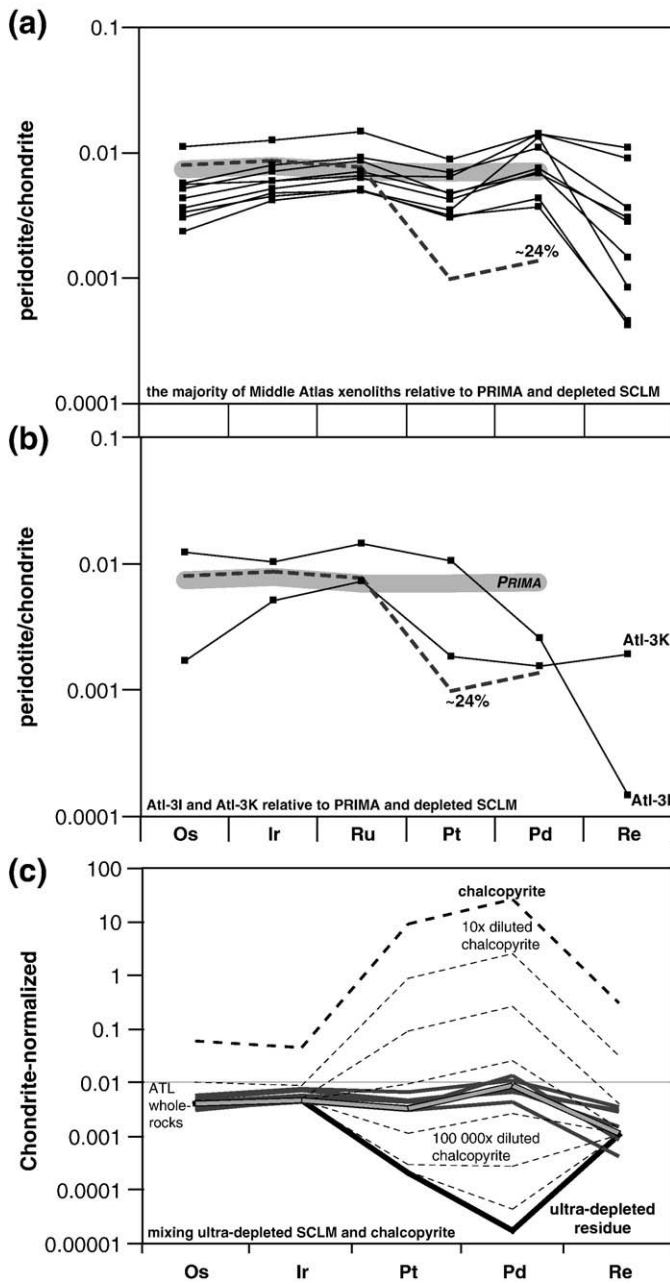


Fig. 8. Chondrite-normalized PGE and Re abundances of whole rock peridotites from Middle Atlas (a and b). Also shown are the patterns of PRIMA (light grey) and a 24% depleted residue (Pearson et al., 2004, dashed). Samples in (a) are marked by increasing abundances from Os through to Ru, low Pt and elevated Pd whereas two samples with distinct PGE patterns are highlighted in (b) (AtI-3I and AtI-3K). In (c), we show the chondrite-normalized PGE patterns of a generic ultra-refractory (sulphide- and clinopyroxene-free) peridotite residue (solid black) and chalcopyrite (black, dashed) with $[Pt/Pd]_N < 1$. We introduce different fractions of chalcopyrite into the depleted peridotite matrix and illustrate the rapid response of the whole rock peridotite PGE systematics to the introduction of secondary magmatic chalcopyrite. This model utilizes chalcopyrite from Barnes et al. (2006) because the PGE systematics of cubanite, mono-sulphide solution, pentlandite and pyrrhotite do not reproduce the Middle Atlas PGE patterns due to their substantially larger fractionation of Pt from Pd. The mixing curves are shown for dilution factors between 10^7 and 10 . Best fit mixing curves that correspond well to the Middle Atlas xenolith PGE systematics are those with a dilution factor of pure chalcopyrite between 1000 and 3000.

The behaviour of sulphides during mantle melting is strongly dependent on pressure and temperature at which melting occurs, the prevalent oxygen fugacity, which determines sulphur solubility in the melt, the FeO content in the melt and also the melt volume (i.e. the degree of melting) that is produced although the exact relationships

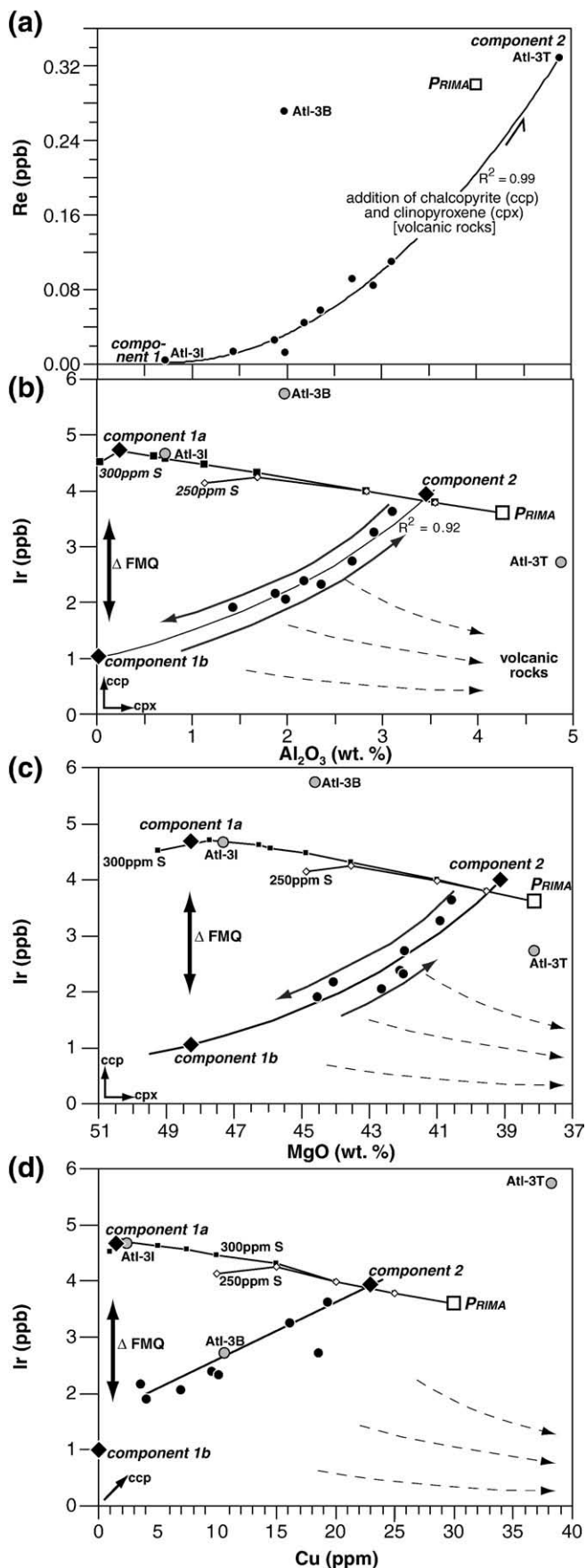
of these factors remain poorly understood (Arndt et al., 2005). In order to observe the ubiquitous P-PGE depletion that is endemic in cratonic SCLM, melt depletion must exceed 20% (Pearson et al., 2004). Furthermore, large-scale melting is required to remove the high-density sulphide portion from the increasingly refractory and therefore buoyant silicate fraction of peridotites.

In the case of the Middle Atlas xenoliths the chondrite-normalized PGE patterns are convex upward with low Os and, to a lesser extent, Ir abundances. They have fractionated $[Os/Ir]_N$ ratios and elevated Pd abundances. With these characteristics the PGE patterns are distinct from a) PRIMA (Becker et al., 2006), b) modelled melt extraction residues based on PRIMA (Lorand et al., 2008) and c) typical magmatic sulphides that are known to occur in SCLM such as pentlandite, cubanite, pyrrhotite and mono-sulphide solid solution (Barnes et al., 2006). For example, in Fig. 7 the total I- and P-PGEs abundances are compared to the melt extraction model of Pearson et al. (2004). The melting evolution of PRIMA is illustrated for residues of 1 to 24% depletion until the sulphide fraction is removed from the residue. This model relies on a PRIMA sulphur content of 250 and 300 ppm and the behaviour of sulphide minerals during melt extraction up to ~24% and 29% depletion with fO_2 conditions encountered during depletion, for example, at mid-ocean ridges. Melting in excess of sulphide consumption cannot be constrained with this model. The majority of Middle Atlas xenoliths are distinctly offset from the depletion trends due to high P-PGE abundances at a given I-PGE content. Consequently, it is difficult to envision a simple one-stage depletion scenario of PRIMA that could account for the observed PGE systematics of these xenoliths. Despite the potential of reconstructing mantle melting using siderophile elements in peridotites in cratons, Alard et al. (2002) and Pearson et al. (2004) (and references therein) have highlighted that secondary sulphide addition may substantially alter PGE systematics in peridotites, and a careful evaluation of Os isotope and PGE elemental systematics is required. Hence, in the light of the PGE systematics of the majority of the Middle Atlas xenoliths some form of metasomatic alteration of the PGE systematics (and possibly Os isotopes) should be anticipated and is discussed in the next section (Section 5.3).

Despite the complexity of the metasomatic activity that effects the PGE systematics in most Middle Atlas xenoliths, a single sample appears to preserve some information on the initial refractory PGE composition. Sample AtI-3I has higher I-PGE abundances relative to the majority of Middle Atlas xenoliths (Fig. 9) and is characterized by depleted major element systematics (Ir versus Al_2O_3 and MgO, Fig. 9). If an initial sulphur content of 300 ppm is present in the source mantle, AtI-3I is tightly associated with the composition anticipated for refractory peridotites after ~25% depletion (Fig. 9). This sample is not only marked by high Ir (and Ru) and MgO, and low Al_2O_3 and Re, it also has very low Cu abundances (Fig. 9). This low Cu content may suggest that melting exceeded 24% and primary base metal sulphides were removed by the melt leading to the precipitation of residual Cu-poor sulphides (e.g., laurite $[Os, Ir, Ru]S_2$, Brenan and Andrews, 2001), which sequester I-PGEs. Notably, the PGE pattern of AtI-3I is similar to the step-like PGE pattern modelled for depleted, cratonic mantle peridotites (Fig. 8) and also to those of laurite and I-PGE-rich alloys (i.e. rutheniridosmine; Cabri, 2002; Shi et al., 2007). The higher Pt abundance in this peridotite may indicate the presence of Pt-rich alloys (Luguet et al., 2007). Therefore, we suggest that the PGE systematics in sample AtI-3I are controlled by laurite and possibly I-PGE-rich alloys and more faithfully record base metal sulphide removal and PGE-rich alloy stabilization due to mantle melting in excess of 25%. We will proceed with investigating the PGE systematics of the remainder of xenoliths in order to better understand the metasomatic evolution in this continental mantle root.

5.3. Exploring PGE-major element trends in the Middle Atlas xenoliths

The majority of samples show perplexingly well-correlated trends of Al_2O_3 , MgO and Cu with Re and Ir (the latter being representative of I-



PGEs), which are not compatible with the residue curves depicted in Fig. 9. We discuss two mechanisms that may influence the PGE systematics in off-cratonic peridotites. First, we discuss the processes of xenolith sampling and entrainment, which have been proposed to dissolve sulphides in some environments causing the fractionation of $[\text{Os}/\text{Ir}]_N$. We also propose a second model based on two mechanisms; the effects of degree of depletion on the Cr- and Mg-contents in spinel and the resulting local depression of $f\text{O}_2$ near Cr-rich spinel. In addition, the changing FeO content of silicate melts resulting from the precipitation of pyroxenes in a dunitic peridotite matrix after melt/rock reaction may affect sulphur saturation of the melt and enable sulphide precipitation.

Handler et al. (1999) proposed the disintegration of sulphides during the eruption of Victoria mantle xenoliths in order to explain the correlation of Cu/S with the fractionated $[\text{Os}/\text{Ir}]_N$ in these peridotites. Such processes have also been suggested to have affected the PGE budget of Vitim peridotites from the Baikal rift (Pearson et al., 2004). We have not determined sulphur contents in the Middle Atlas xenoliths, however, Cu abundances do correlate well with Re, Os and particularly Ir in addition to MgO and Al_2O_3 . Such well-defined trends are absent in the Australian xenoliths studied by Handler et al. (1999). Major element mobility is unlikely to be induced by the disintegration of sulphides during eruption. Therefore, the breakdown of sulphides during eruption and preferential removal of Os via volatilization is a less likely process to have substantially affected the Middle Atlas xenoliths and a melting or metasomatic event linking PGEs and major elements is needed.

5.3.1. Small scale $f\text{O}_2$ variability associated with depletion and sulphide precipitation during silicate melt metasomatism

With our second approach, we seek one model that may explain the PGE-major element systematics of all Middle Atlas SCLM xenoliths. Two mechanisms that operate at centi- to meter-scale and are the consequence of melting and metasomatic processes in the Earth's upper mantle may substantially influence the prevalent $f\text{O}_2$. This in turn effects the solubility of sulphides in silicate melts and also the efficiency of I-PGE-rich alloy formation in refractory peridotites regardless of the tectonic setting in which melting occurs (i.e. MOR versus subduction zone). These processes may therefore reconcile the low PGE abundances in the Middle Atlas xenoliths, the correlation of the major elements with I-PGEs, Re and also Os isotopes exhibited in the majority of samples as well as the MOR-like ΔNNO determined by V-Sc systematics.

Fig. 9. Comparison of Re (a) and Ir abundances (ppb) versus Al_2O_3 (wt.%, b), MgO (inverse axis, wt.%, c) and Cu (ppm, d) shown in comparison to PRIMA. In (b) to (d) two depletion trends assuming 250 and 300 ppm S in PRIMA are shown. Under low $f\text{O}_2$, MOR-like conditions melting increases Ir abundances and decreases Re, Al_2O_3 , MgO and Cu. Also shown in (b) to (d) are vectors of chalcopyrite (ccp) and clinopyroxene (cpx) addition. The dashed arrows indicate the composition of volcanic rocks (high Al_2O_3 and Cu with low MgO and Ir). Samples AtI-3I, AtI-3I and AtI-3B are highlighted as grey circles from the majority of samples (black circles). Note that in Re– Al_2O_3 (a) all samples except AtI-3B are extremely well-correlated ($R^2 = 0.99$, linear trend); if AtI-3I is excluded the mathematical correlation is only mildly impaired ($R^2 = 0.94$). In Ir– Al_2O_3 , MgO and Cu space, the harzburgite AtI-3I is associated with compositions associated with mantle melting in low $f\text{O}_2$ conditions if 300 ppm sulphur is assumed for PRIMA (PRIMA to component 1a). However, the majority of Middle Atlas samples are marked by well-correlated Ir-major element systematics although Ir abundances are low relative to the modelled melting trends. This Ir-major element correlation most likely results from depletion to the degree of complete sulphide–clinopyroxene exhaustion without significant alloy stabilization due to the lower Cr-component in spinel and the lack of $f\text{O}_2$ depression adjacent to the spinel during the course of melting (Mungall, 2005). The resulting variable Ir abundances (components 1a to 1b) and the refractory major element systematics are altered during the coupled introduction of secondary sulphides and clinopyroxenes, which is possible if the precipitation of pyroxenes drives the silicate melt volume above sulphur saturation (Lorand et al., 2003) (components 1a and 1b to 2). Two exceptions, which are not associated with the variable $f\text{O}_2$ melting and modal metasomatism trends of the majority of samples are AtI-3T and AtI-3B. These samples may be reconciled with extreme depletion and later modal metasomatism that is dominated by sulphide, possibly chalcopyrite (ccp), and clinopyroxenes, respectively.

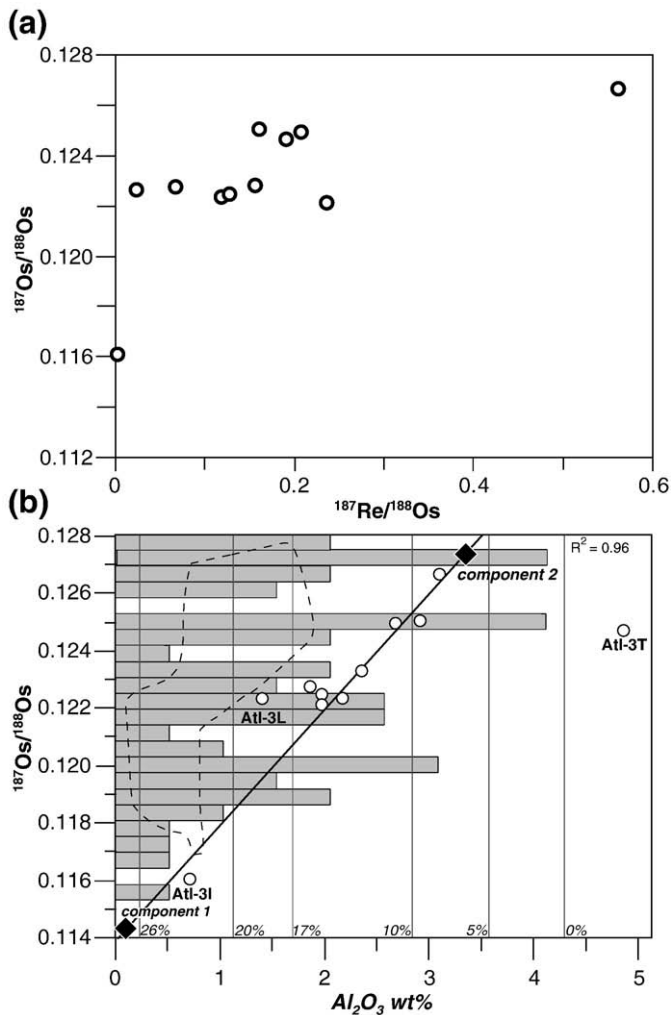


Fig. 10. $^{187}\text{Os}/^{188}\text{Os}$ versus $^{187}\text{Re}/^{188}\text{Os}$ (a) and Al_2O_3 (wt.%) (b) of Middle Atlas whole rock peridotites. Note the lack of isochronous correlation in (a). $^{187}\text{Os}/^{188}\text{Os}$ – Al_2O_3 of whole rock peridotites from Middle Atlas mantle xenoliths are tightly correlated if samples Atl-3T and Atl-3L are ignored on the basis of their elevated Al_2O_3 (wt.%) and radiogenic Os, respectively. Also shown are the $^{187}\text{Os}/^{188}\text{Os}$ – Al_2O_3 relationships of abyssal peridotites (dashed field, Becker et al., 2006; Harvey et al., 2006) and the $^{187}\text{Os}/^{188}\text{Os}$ histogram of abyssal peridotites is taken from Pearson et al. (2007 and references therein). The degree of depletion (vertical lines in per cent (a)) is estimated from Al_2O_3 contents (polybaric melting at ~2 GPa after Herzberg, 2004). This positive Os isotope–Al correlation most likely results from a two-component mixing process of a highly depleted component with relatively unradiogenic Os isotopes akin to Atl-3L and PRIMA-like mantle.

First, we note the systematic difference in I-PGE abundances in peridotites from on- and off-cratonic xenoliths, which have higher and lower (or similar) I-PGEs relative to PRIMA, respectively. The overall higher I-PGE abundances of cratonic SCLM may be related to the degree of melting, which is assumed to reach 30 to 40%, resulting in the complete removal of sulphides. Whole rock PGE patterns of these peridotites are identical to I-PGE-rich alloys (Pearson et al., 2007). The constituent spinels in these ultra-refractory peridotites are close to the chromite endmember and therefore dominated by Al and, importantly, the redox-sensitive $\text{Fe}^{2+,3+}$ and especially $\text{Cr}^{2+,3+}$ at the expense of MgO (e.g., Bernstein et al., 2006). Although variable, cratonic spinels have Cr# and MgO between 50–99 and 10–16 wt.% (e.g., Bizzarro and Stevenson, 2003; Simon et al., 2003). Mungall (2005) proposed that the spinel crystal structure appears to disproportionately incorporate Fe^{3+} and Cr^{3+} and thus with continued melting to ~40%, the removal of these oxidised elements from the melt causes the local enrichment of Fe^{2+} and Cr^{2+} in the melt and the depression of the $f\text{O}_2$ in the vicinity of the growing spinel crystal. This compositional boundary layer with low $f\text{O}_2$

should become more pronounced with the increasing degree of melting, i.e. the increasing Cr content in spinel. Experimental studies suggest that this localized reduction of $f\text{O}_2$ may induce the stabilization of I-PGE-rich alloys (micro-nuggets) adjacent to spinel-chromite crystals (Mungall, 2005). Eventually, these alloys may be overgrown by the chromite and efficiently protected from metasomatic agents that percolate in the SCLM. With the stabilization and protection of I-PGE-rich alloy inclusions in chromite, the refractory whole rock PGE abundances in on-cratonic peridotites become elevated relative to PRIMA and preserved during metasomatism in the course of SCLM evolution.

In the case of off-cratonic SCLM, melt extraction appears to not exceed 30%, thus spinel in these peridotites is substantially more Mg-rich and Cr-poor (Middle Atlas spinel Cr# = 15–33, MgO = 18–22 wt.%, Wittig, 2006). The low $f\text{O}_2$ zone adjacent to the spinel is unlikely to become established and hence this lower Cr content does not facilitate the formation of I-PGE alloys. As such the complete exhaustion of sulphides, including laurite, would allow the partial removal of I-PGEs from the residue, thereby effectively lowering PGE abundances in off-cratonic SCLM such as that from the Middle Atlas.

Secondly, the good correlations of Re, Ir and Os isotopes with Al_2O_3 , MgO and Cu of the Middle Atlas xenoliths may result from the precipitation (≤ 5 wt.% FeO, Wittig, 2006) at the expense of olivine (~8 to 12 wt.% FeO) from a silicate melt (Yi et al., 2000; Lorand et al., 2003). This process may result in a decreasing melt volume and the relative increase of sulphur concentrations in the melt, which in turn drives the silicate melt toward S-saturation. At this point sulphides precipitate in conjunction with the pyroxenes and amphibole. Contemporaneous introduction of sulphides and clinopyroxene has also been reported from off-craton xenoliths from Sidamo, Ethiopia (Lorand et al., 2003). This model gains further support from the Os isotope correlation with major elements, which suggests that this compositional and isotope variation may result from a two-component mixing process of a substantially depleted component with variable I-PGE contents (components 1a and 1b) with a more fertile component (component 2, Fig. 10), which is marked by more radiogenic Os, higher Al_2O_3 , SiO₂, Re, I-PGEs, Cu, Sc, and V and lower MgO, FeO and Ni (Figs. 3–7 and 9–10). Samples Atl-3B and Atl-3T, which fall distinctly off the mixing trends in Fig. 9 may have acquired their relatively high Ir (Atl-3B) and Al_2O_3 (Atl-3T) from the predominant crystallization of sulphide and clinopyroxene, respectively, while the majority of samples appear to have experienced a more balanced and coupled introduction of sulphide and clinopyroxene.

It is important to test this model which proposes substantial depletion of all samples and the coupled introduction of sulphide and clinopyroxene/amphibole with regard to P-PGE abundances and the entire PGE systematics of the Middle Atlas xenoliths. We model the PGE systematics of the Middle Atlas xenoliths by assuming a highly depleted peridotite into which small fractions of magmatic sulphides are being mixed in. Here, good agreement of the PGE patterns of the Middle Atlas xenoliths can be achieved if small fractions of chalcopyrite with $[\text{Pt}/\text{Pd}] < 1$ are mixed back into the putative residue (Fig. 8). The PGE systematics of cubanite, mono-sulphide solution, pentlandite and pyrrhotite (Barnes et al., 2006) do not reproduce the Middle Atlas PGE patterns due to their substantially larger fractionation of Pt from Pd. Chalcopyrite has the highest Cu abundances of the most common magmatic sulphides and the well established trends of Ir and major elements with Cu in the Middle Atlas xenoliths further support the predominant introduction of minute amounts of chalcopyrite. Assuming all Cu is hosted by chalcopyrite the modal abundances of this sulphide amounts to only a fraction of a percent (0.01% Atl-3B and 0.001% Atl-3L). These very low chalcopyrite abundances are consistent with the general lack of observable sulphides in the thin section. Despite the good fit of the chalcopyrite it should be noted that the PGE patterns of the Middle Atlas peridotites most likely host a more complex assemblage of magmatic sulphides, which is difficult to recreate in our models.

As such, we propose that the initial depletion of all samples occurred under somewhat low f_{O_2} conditions evolving along the depletion trend from the composition of PRIMA producing a highly refractory harzburgitic residue with low Al_2O_3 and Cu and high MgO similar to Atl-3I (Fig. 9). Melting may have continued, although the chromite-component in spinel remains low relative to cratonic spinel, thus the stabilization of alloys may have been inhibited and the I-PGEs abundances in the residue decrease during continued melting. Later, the harzburgitic to dunitic SCLM underwent silicate melt/rock reaction introducing sulphides and clinopyroxenes/amphibole establishing the correlation of I-PGEs and major elements.

This sequence of events also predicts that the clinopyroxene now present in the studied portion of the Middle Atlas SCLM is nearly entirely of secondary origin as a result of melt/dunite reaction. It is also noteworthy that these constituent clinopyroxenes are marked by elevated lithophile trace element abundances and fractionated ratios of elements with similar incompatibility and behaviour during silicate melting and metasomatism (e.g. Zr/Hf and U/Nb) suggesting that the trace element systematics as well as Sr–Nd–Hf–Pb isotope systematics result from metasomatic enrichment due to interaction with carbonatitic liquids. Carbonatites are assumed to be largely devoid of PGEs (Chesley et al., 2004) and therefore interaction with such liquids does not appear to provide a relevant mechanism to explain the observed PGE systematics of the Middle Atlas xenoliths. Following from this, lithophile elemental and Sr–Nd–Hf isotope systematics determined from clinopyroxene from the Middle Atlas (Wittig et al., in press) along with whole rock siderophile element systematics presented here suggest that at least two metasomatic events can be distinguished in the Middle Atlas xenoliths. First, passing silicate melts lead to the precipitation of clinopyroxene and/or amphibole plus the introduction of magmatic sulphides into a more refractory harzburgite–dunite matrix establishing the PGE-major element correlations. Later and close to the time of eruption of the host volcanic rocks, carbonatitic liquids imposed radiogenic Pb isotope ratios and high U/Pb, Th/Pb as well as Th/U in addition to HIMU-like Sr–Nd–Hf isotopes onto the previously precipitated diopsidic clinopyroxenes (Wittig et al., in press). These events may broadly relate to the initial rifting during the Triassic–Jurassic, which is associated with basaltic volcanism and the younger Miocene intraplate volcanic activity during which carbonatitic liquids appear to have percolated through the lithosphere. Unfortunately, the Os isotope composition of magmatic rocks derived from these events is unknown. Overall, major element and PGE systematics of the Middle Atlas SCLM record metasomatism and the depletion signature is substantially masked.

5.4. What can we say about the age of the continental mantle root of the Middle Atlas?

We are in the possession of a comprehensive dataset for the Middle Atlas xenoliths that comprises five radiogenic isotope systems, whole rock and mineral major elements in addition to lithophile and siderophile trace element data. In this contribution we have explored the origin of the well-correlated major elements, PGE abundances and Os isotope ratios, which most likely result from melt/rock reaction and precipitation of sulphides together with clinopyroxenes and/or amphibole after initial melting had removed primarily sulphides and clinopyroxenes. None of the lithophile and siderophile isotope systems yield meaningful isochronous parent–daughter relationships or model ages that provide information on the timing of depletion or SCLM stabilization. However, some constraints regarding the initial depletion are important to consider.

The T_{RD} Os model age of the least radiogenic sample yields a minimum age of 1.7 Gyr. Our view is that it is unwise to use either of these ages as an indication of the age of the lithospheric mantle beneath the Middle Atlas. This is because even the age of the least radiogenic sample is within the $^{187}Os/^{188}Os$ range shown by abyssal peridotites

(Becker et al., 2006; Harvey et al., 2006) and Pt alloy samples (Meibom et al., 2002; Pearson et al., 2007) derived from oceanic lithosphere (Fig. 10). This allows the possibility of more recent incorporation of oceanic mantle in this area to form a continental mantle root. Such a root may contain a fraction of peridotites with 1.7 Gyr T_{RD} ages. The diffuse spread of $^{187}Os/^{188}Os$ ratios has a mode of around 0.124. This $^{187}Os/^{188}Os$ presents an offset from present-day chondrite that only accounts for 1 Myr. Because of the severe distribution of the PGE budget of these xenoliths and their very scattered Os isotope ratios we consider it unwise to use any of the Os isotope data to propose an age for the bulk of the continental mantle root. The prospect of using other isotope systems such as Lu–Hf is not bright as initial studies indicate that these systems are also significantly disturbed (Wittig et al., in press). Clearly these samples evolved together, but whether this occurred in the continental mantle root beneath the Middle Atlas, or within the convecting mantle cannot be determined.

6. Conclusions

We have investigated a suite of variably metasomatised spinel peridotites from the Middle Atlas of Morocco.

- (1) FeO–MgO and Sc–V elemental systematics are indicative of minimal depletion; although a single sample suggests ~25% melt depletion.
- (2) Unlike FeO and MgO, SiO_2 – Al_2O_3 systematics are substantially different from melt residues and suggest either amphibole-, Al-rich clinopyroxene- or diopsidic clinopyroxene-spinel-addition leaving Al abundances notably enriched.
- (3) PGE systematics in the majority of peridotites are substantially fractionated and appear to stem from the introduction of magmatic sulphides. PGE systematics indicative of mantle melting can only be found in one refractory xenolith.
- (4) Os isotope ratios in Middle Atlas xenoliths are variable; nonetheless the range is within that of the convecting mantle. Most samples cluster at $^{187}Os/^{188}Os \sim 0.122$, although a single sample with the most refractory major element systematics has $^{187}Os/^{188}Os$ of 0.117.
- (5) An Al_2O_3 –Os isotope correlation yields a Paleoproterozoic stabilization age for the Middle Atlas SCLM. However, the extent of metasomatism suggests contemporaneous introduction of secondary sulphides, clinopyroxene-spinel and/or amphibole whereby Al contents and Os isotopes became coupled. Hence, it is unlikely that Al–Os relations can be used to constrain the SCLM age.
- (6) Fundamentally, major elements and PGE elemental and Os isotope systematics of the Middle Atlas xenoliths are severely influenced by metasomatic alteration that occurred subsequent to an initial mantle melting event. Application of lithophile and siderophile isotope systems fails to provide age information for this portion of the SCLM.

Acknowledgements

This study was supported by a Natural Environment Research Council grant to DGP (NERC, UK, NE/C5/9054/1) and also benefited in its initial stages from funding provided by the Danish National Research Foundation to the Danish Lithosphere Centre. S.D. was supported by the German Research Foundation (DFG grant Ho1833/18-1) and the guidance and help of A. Moukadiri and P. van de Bogaard during fieldwork is appreciated. NW wishes to express gratitude to Bill Waterson for, amongst other things, key observations on the ballistic properties of rocks, the joys of imaginary numbers and sunny fields, which ultimately helped to finish this manuscript. Chris J. Ottley and Chris W. Dale are thanked for help with Asher digestion procedures and Os isotope and PGE concentration measurements. G. Fitton is thanked for handling XRF analyses in Edinburgh. Special thanks to the

inhabitants of R136 in DH: Akira Ishikawa for advice and discussions, sharing Asher insights, and, above all, regular coffee breaks while Joanne Peterkin and Ali Rogers are credited for good company and being jolly and pun. We are also thankful for discussions with Nick T. Arndt concerning the melting of sulphides and (in-)compatibility of PGEs. The detailed reviews by R.J. Walker and L. Reisberg are extremely appreciated and helped to further explore some of the ideas presented.

References

- Alard, O., Griffin, W.L., Pearson, N.J., Lorand, J.-P., O'Reilly, S.Y., 2002. New insights into the Re–Os systematics of sub-continental lithospheric mantle from in situ analysis of sulfides. *Earth and Planetary Science Letters* 203, 651–663.
- Arndt, N.T., Leshner, C.M., Czamanske, G.K., 2005. Mantle-derived magmas and magmatic Ni–Cu–(PGE) deposits. *Economic Geology* 100th Anniversary Volume, pp. 5–23.
- Ayarza, P., Alvarez-Lobato, F., Teixell, A., Arboleya, M.L., Tesón, E., Julivert, M., Charroud, M., 2005. Crustal structure under the High Atlas Mountains (Morocco) from geological and gravity data. *Tectonophysics* 400, 67–84.
- Ban, M., Witt-Eickschen, G., Klein, M., Seck, H.A., 2005. The origin of glasses in hydrous mantle xenoliths from the West Eifel, Germany: incongruent break-down of amphibole. *Contributions to Mineralogy and Petrology* 148, 511–523.
- Barnes, S.-J., Cox, R.A., Zientek, M.L., 2006. Platinum-group element, gold, silver, and base metal distribution in compositionally zoned sulphide droplets from the Medvezky Creek Mine, Noril'sk, Russia. *Contributions to Mineralogy and Petrology* 152, 187–200.
- Beauchamp, W., Barazangi, M., Demnati, A., El Alji, M., 1996. Intracontinental rifting and inversion: Missour Basin and Atlas Mountains, Morocco. *AAPG Bulletin* 80 (9), 1459–1482.
- Becker, H., Horan, M.F., Walker, R.J., Gao, S., Lorand, J.-P., Rudnick, R.L., 2006. Highly siderophile element composition of the Earth's primitive upper mantle: constraints from new data on peridotite massifs and xenoliths. *Geochimica et Cosmochimica Acta* 70, 4528–4550.
- Bernstein, S., Hanghøj, K., Kelemen, P.B., Brooks, C.K., 2006. Ultra-depleted, shallow cratonic mantle beneath West Greenland: dunitic xenoliths from Ubekendt Eiland. *Contributions to Mineralogy and Petrology* 152, 335–347.
- Bizzarro, M., Stevenson, R.K., 2003. Major element composition of the lithospheric mantle under the North Atlantic craton: evidence from peridotite xenoliths of the Sarfartoq area, southwest Greenland. *Contributions to Mineralogy and Petrology* 146, 223–240.
- Brenan, J.M., Andrews, D., 2001. High temperature stability of laurite and Ru–Os–Ir alloy and their role in PGE fractionation in mafic magmas. *Canadian Mineralogist* 39, 341–360.
- Cabri, L.J., 2002. The platinum-group minerals. In: Cabri, L.J. (Ed.), *The Geology, Geochemistry, Mineralogy and Mineral Beneficiation of Platinum-Group Elements*: Canadian Institute of Mining, Metallurgy and Petroleum, Special Volume 54, pp. 13–129.
- Canil, D., 2002. Vanadium in peridotites, mantle redox and tectonic environments: Archean to present. *Earth and Planetary Science Letters* 195, 75–90.
- Canil, D., 2004. Mildly incompatible elements in peridotites and the origins of mantle lithosphere. *Lithos* 77 (1–4), 375–393.
- Chesley, J., Richter, K., Ruiz, J., 2004. Large-scale mantle metasomatism: a Re–Os perspective. *Earth and Planetary Science Letters* 219, 49–60.
- Dale, C.W., Luguet, A., Macpherson, C.G., Pearson, D.G., Hickey-Vargas, 2008. Extreme platinum-group element fractionation and variable Os isotope compositions in Philippine Sea Plate basalts: tracing mantle source heterogeneity. *Chemical Geology* 248, 213–238.
- Duggen, S., Hoernle, K., van den Bogaard, P., Ruepke, L., Morgan, J.P., 2003. Deep roots of the Messinian salinity crisis. *Nature* 422, 602–604.
- Duggen, S., Hoernle, K., Hauff, F., Kluegel, A., Bouabdellah, M., Thirlwall, M.F., 2009. Flow of Canary mantle plume material through a subcontinental lithospheric corridor beneath Africa to the Mediterranean. *Geology* 37, 283–286.
- Gomez, F., Allemendiger, R., B., M., Er-Raji, A., Dahmani, M., 1998. Crustal shortening and vertical strain partitioning in the Middle Atlas Mountains of Morocco. *Tectonics* 17, 520–533.
- Handler, M.R., Bennett, V.C., 1999. Behaviour of platinum-group elements in the subcontinental mantle of eastern Australia during variable metasomatism and melt depletion. *Geochimica et Cosmochimica Acta* 63, 3597–3618.
- Handler, M.R., Bennett, V.C., Dreibus, G., 1999. Evidence from correlated Ir/Os and Cu/S for late-stage Os mobility in peridotite xenoliths: implications for Re–Os systematics. *Geology* 27, 75–78.
- Harvey, J., Abdelmouhcine Gannoun, A., Burton, K.W., Rogers, N.W., Alard, A., Parkinson, I.J., 2006. Ancient melt extraction from the oceanic upper mantle revealed by Re–Os isotopes in abyssal peridotites from the mid-Atlantic ridge. *Earth and Planetary Science Letters* 244, 606–621.
- Herzberg, C., 2004. Geodynamic information in peridotite petrology. *Journal of Petrology* 45, 2507–2530.
- Ionov, D.A., Hofmann, A.W., 2007. Depth of formation of subcontinental off-craton peridotites. *Earth and Planetary Science Letters* 261, 620–634.
- Irvine, G.J., Pearson, D.G., Carlson, R.W., 2001. Lithospheric mantle evolution in the Kaapvaal craton: a Re–Os isotope study of peridotite xenoliths from Lesotho kimberlites. *Geophysical Research Letters* 28, 2505–2508.
- Irvine, G.J., Pearson, D.G., Kjarsgaard, B.A., Carlson, R.W., Kopylova, M.G., Dreibus, G.E., 2003. A Re–Os isotope and PGE study of kimberlite-derived peridotite xenoliths from Somerset Island and a comparison to the Slave and Kaapvaal craton. *Lithos* 71, 461–488.
- Kelemen, P.B., Hart, S., Bernstein, S., 1998. Silica enrichment in the continental upper mantle via melt/rock reaction. *Earth and Planetary Science Letters* 164, 387–406.
- Kopylova, M.G., Russell, J.K., 2000. Chemical stratification of cratonic lithosphere: constraints from the Northern Slave craton, Canada. *Earth Planet. Sci. Lett.* 181, 71–87.
- Krushevskaya, A.P., Zhou, Y., Ravikumar, V., Y.-J., K., Hinrichs, J., 2006. Chromium based polyatomic interferences on rhodium in ICP-MS. *Journal of Analytical Atomic Spectrometry* 21, 847–855.
- Lorand, J.-P., Reisberg, L., Bedini, R.M., 2003. Platinum-group elements and melt percolation in Sidamo spinel peridotite xenolith, Ethiopia, East African Rift. *Chemical Geology* 196, 57–75.
- Lorand, J.-P., Luguet, A., Alard, A., 2008. Platinum-group elements: a new set of key tracers for the Earth's interior. *Elements* 4, 247–252.
- Luguet, A., Shirey, S.B., Lorand, J.-P., Horan, M.F., Carlson, R.W., 2007. Residual platinum-group minerals from highly depleted harzburgites of the Lherz massif (France) and their role in HSE fractionation of the mantle. *Geochimica et Cosmochimica Acta* 71, 3082–3097.
- Luguet, A., Nowell, G.M., Pearson, D.G., 2008. $^{184}\text{Os}/^{188}\text{Os}$ and $^{186}\text{Os}/^{188}\text{Os}$ measurements by negative thermal ionisation mass spectrometry (N-TIMS): effects of interfering element and mass fractionation corrections on data accuracy and precision. *Chemical Geology* 248, 342–362.
- McDonough, W.F., Sun, S.-s., 1995. The composition of the Earth. *Chemical Geology* 120, 223–253.
- Meibom, A., Sleep, N.H., Chamberlain, C.P., Coleman, R.G., Frei, R., Hren, M.T., Wooden, J.L., 2002. Re–Os isotopic evidence for long-lived heterogeneity and equilibration processes in the upper mantle. *Nature* 419, 705–708.
- Meisel, T., Walker, R.J., Morgan, J.W., 1996. The osmium isotopic composition of the Earth's primitive upper mantle. *Nature* 383, 517–520.
- Meisel, T., Moser, J., Kettisch, P., 2008. Determination of Osmium and Other Platinum Group Elements in Chromitites by Acid Digestion and ICP-MS. Department of General and Analytical Chemistry, University of Leoben, Leoben, p. 1.
- Mungall, J.E., 2005. Magmatic geochemistry of the platinum-group elements. In: Mungall, J.E. (Ed.), *Exploration of Platinum-Group Element Deposits*. Mineralogical Association of Canada (short course), Oulu, Finland.
- Pearson, D.G., Woodland, S.J., 2000. Carius tube digestion and solvent extraction/ion exchange separation for the analysis of PGE's (Os, Ir, Pt, Pd, Ru) and Re–Os isotopes in geological samples by isotope dilution ICP-mass spectrometry. *Chemical Geology* 165, 87–107.
- Pearson, D.G., Wittig, N., 2008. Formation of Archaean continental lithosphere and its diamonds: the root of the problem. *Journal of the Geological Society* 165, 895–914.
- Pearson, D.G., Davies, G.R., Nixon, P.H., 1993. Geochemical constraints on the petrogenesis of diamond facies pyroxenites from the Beni Bousera Massif, North Morocco. *Journal of Petrology* 34 (1), 125–172.
- Pearson, D.G., Snyder, G.A., Shirey, S.B., Taylor, L.A., Carlson, R.W., Sobolev, N.V., 1995. Archaean Re–Os age for Siberian eclogites and constraints on Archaean tectonics. *Nature* 374, 711–713.
- Pearson, D.G., Irvine, G.J., Ionov, D.A., Boyd, F.R., Dreibus, G.E., 2004. Re–Os isotope systematics and platinum group element fractionation during mantle melt extraction: a study of massif and xenolith peridotite suites. *Chemical Geology* 208, 29–59.
- Pearson, D.G., Parman, S.W., Nowell, G.M., 2007. A link between large mantle melting events and continent growth seen in osmium isotopes. *Nature* 449, 202–205.
- Priestley, K., McKenzie, D., 2006. The thermal structure of the lithosphere from shear wave velocities. *Earth and Planetary Science Letters* 244, 285–301.
- Ramandi, F., 1998. Geodynamic implications of intermediate-depth earthquakes and volcanism in the intraplate Atlas Mountains (Morocco). *Physics of the Earth and Planetary Interiors* 108, 245–260.
- Reisberg, L., Lorand, J.-P., 1995. Longevity of sub-continental mantle lithosphere from osmium isotope systematics in orogenic peridotite massifs. *Nature* 376, 159–162.
- Rudnick, R.L., Walker, R.J., 2009. Interpreting ages from Re–Os isotopes in peridotites. *Lithos* 112 (2), 1083–1095.
- Shi, R., Alard, O., Zhi, X., O'Reilly, S.Y., Pearson, N., Griffin, W.L., Zhang, M., Chen, X., 2007. Multiple events in the Neo-Tethyan oceanic upper mantle: evidence from Ru–Os–Ir alloys in the Luobusa and Dongqiao ophiolitic podiform chromitites, Tibet. *Earth and Planetary Science Letters* 261, 33–48.
- Simon, N.S.C., Irvine, G.J., Davies, G.R., Pearson, D.G., Carlson, R.W., 2003. The origin of garnet and clinopyroxene in “depleted” Kaapvaal peridotites. *Lithos* 71, 289–322.
- Streckeisen, A., 1976. To each plutonic rock its proper name. *Earth Science Reviews* 12, 1–33.
- Teixell, A., Arboleya, M.L., Julivert, M., Charroud, M., 2003. Tectonic shortening and topography in the central High Atlas (Morocco). *Tectonics* 22 (5), 1051.
- Walker, R.J., Carlson, R.W., Shirey, S.B., Boyd, F.R., 1989. Os, Sr, Nd, and Pb isotope systematics of southern African peridotite xenoliths: implications for the chemical evolution of subcontinental mantle. *Geochimica et Cosmochimica Acta* 53, 1583–1595.
- Walter, M.J., 1999. Melting residue of fertile peridotite and the origin of cratonic lithosphere. In: Fei, Y., Bertka, C.M., Mysen, B.O. (Eds.), *Mantle Petrology: Field Observations and High Pressure Experimentation*. Spec. Pub. Geochem. Soc. Houston, vol. 6, pp. 225–239.
- Walter, M.J., 2003. Melt extraction and compositional variability in mantle lithosphere. In: Holland, H.D., Turekian, K.K. (Eds.), *Treatise on Geochemistry*. Elsevier, pp. 363–394.
- Wittig, N., 2006. Application of Novel U–Th–Pb and Lu–Hf Isotopic Techniques to Tracing the Melting and Metasomatic History of Mantle Rocks. University of Copenhagen, Copenhagen. 352 pp.
- Wittig, N., Pearson, D.G., Baker, J.A., Duggen, S., Hoernle, K., 2008a. Young continental mantle root beneath the Middle Atlas, Morocco: evidence for carbonatite metasomatism. 9th International Kimberlite Conference Extended Abstract No. 9IKC-A-00268, pp. 1–3.

- Wittig, N., Pearson, D.G., Webb, M., Ottley, C.J., Irvine, G.J., Kopylova, M.G., Jensen, S.M., Nowell, G.M., 2008b. Origin of cratonic lithospheric mantle roots: a geochemical study of peridotites from the North Atlantic Craton, West Greenland. *Earth and Planetary Science Letters* 274, 24–33.
- Wittig, N., Pearson, D.G., Duggen, S., Baker, J.A., Hoernle, K., in press. Tracing the metasomatic and magmatic evolution of continental mantle roots with Rb–Sr, Sm–Nd Lu–Hf and U–Th–Pb isotopes: A case study of Middle Atlas (Morocco) peridotite xenoliths. *Geochimica et Cosmochimica Acta*. doi:10.1016/j.gca.2009.10.048.
- Yi, W., Halliday, A.N., Alt, J.C., Lee, D.-C., Rehkämper, M., 2000. Cadmium, indium, tin, tellurium and sulphur in oceanic basalts: implications for chalcophile element fractionation in the Earth. *Journal of Geophysical Research* 105 (B8), 18,927–18,948.
- Zeyen, H., Ayarza, P., Fernández, M., Rimi, A., 2005. Lithospheric structure under the western African European plate boundary: a transect across the Atlas Mountains and the Gulf of Cadiz. *Tectonics* 24 (2). doi:10.1029/2004TC001639.